Optimal edge termination for high oxide reliability aiming 10kV SiC n-IGBTs

Perkins, S, Antoniou, M, Tiwari, AK, Arvanitopoulos, A, Gyftakis, KN, Trajkovic, T, Udrea, F & Lophitis, N

DOI 10.1109/DEMPED.2019.8864919

Publisher: IEEE

Optimal edge termination for high oxide reliability aiming 10kV SiC n-IGBTs

S. Perkins, M. Antoniou, Amit K. Tiwari, A. Arvanitopoulos, K. N. Gyftakis,
T. Trajkovic, F. Udrea, N. Lophitis.

***Abstract*— The edge termination design strongly affects the ability of a power device to support the desired voltage and its reliable operation. In this paper we present three appropriate termination designs for 10kV n-IGBTs which achieve the desired blocking requirement without the need for deep and expensive implantations. Thus, they improve the ability to fabricate, minimise the cost and reduce the lattice damage due to the high implantation energy. The edge terminations presented are optimised both for achieving the widest immunity to dopant activation and to minimise the electric field at the oxide. Thus, they ensure the long-term reliability of the device. This work has shown that the optimum design for blocking voltage and widest dose window does not necessarily give the best design for reliability. Further, it has been shown that Hybrid Junction Termination Extension structure with Space Modulated Floating Field Rings can give the best result of very high termination efficiency, as high as 99%, the widest doping variation immunity and the lowest electric field in the oxide.**

Index Terms — IGBT, Oxide, Performance, Reliability, Silicon Carbide, Termination, UHV.

I. INTRODUCTION

Significant progress has been made in the development of Silicon Carbide (SiC) >10kV IGBT devices[1]–[4], yet, no commercial 4H-SiC Ultra High Voltage (UHV) IGBTs are currently available. The presence of large quantities of defects including micropipes, dislocations, stacking faults, fixed charges at the Silicon Dioxide (SiO_2) interface and growth difficulties has obstructed commercial realization [5], [6]. Nevertheless, with continuing growth refinements and design improvements, 4H-SiC MOS based devices are now widely available at up to 1.7kV.

Increased challenges due to 4H-SiC's high critical electric field (2~3 $MVcm^{-1}$) [7] have placed considerable concern for the reliability of the oxide/insulator. The critical electric field of intrinsic SiO_2 is ~10 $MVcm^{-1}$, however, it is advisable to suppress the electric field in SiO_2 below 4 $MVcm^{-1}$ [8], particularly when considering devices for elevated temperatures and large oxide layers, whose failure is dictated by extrinsic failures [9] and therefore, may suffer premature Time Dependent Dielectric Breakdown (TDDB).

The suppression of this electric field in SiC UHV power devices enables the necessary blocking voltage (V_{br}) for functional use to be achieved. For practical power devices, the three-Dimensional junction curvature effect needs to be addressed and substantially suppressed to achieve a high V_{br}. The complexity of termination designs is further exacerbated by virtually no diffusion of impurities in SiC which in turn makes the formation of deep and graded junctions impossible [10]. Consequently, the main blocking junction is in a closer vicinity to the interface with the oxide and in addition the curvature effects can become more intense. This is subsequently, intensified when higher blocking voltages are targeted, e.g. for UHV devices, where the electrostatic potential needs to be supported along thicker and wider semiconductor regions.

Although, several authors have demonstrated promising edge termination designs for UHV SiC power devices including bevel junctions, Junction Termination Extension (JTE), Floating Field Rings (FFR) and hybrid JTE Space Modulated Floating Field Rings (JTE SM-FFR) designs [11]–[15], few works have been conducted which analyze the electric field within the termination oxide.

In this paper we performed extensive and systematic Technology Computer Aided Design (TCAD) modelling and simulations with scope to identify and analyse the UHV termination techniques for 4H-SiC n-channel IGBTs. To ensure accurate results, the physics parameter set of 4H-SiC was updated and a comprehensive list of physics models were used. Further, the impact of those termination designs on the electric field at the oxide is studied and the termination is optimised to achieve the widest possible immunity to dose variations whilst at the same time to keep the electric field at the oxide minimal. The latter would guarantee high reliability, reduced field emission and hot carrier injection. All termination designs are making use of shallow implants, i.e. those which can be achieved with implantation energies lower than 800 keV.

S. Perkins, A. Arvanitopoulos and N. Lophitis are with the Institute for Future Transport and Cities, Coventry University, Coventry, CV1 2HJ, UK. (e-mail: n.lophitis@coventry.ac.uk).
K. N. Gyftakis is with the School of Engineering, University of Edinburgh, UK (e-mail: k.n.gyftakis@ieee.org).
M. Antoniou is with the School of Engineering, University of Warwick, Coventry, UK (e-mail: marina.antoniou@warwick.ac.uk).
A. K. Tiwari, T. Trajkovic and F. Udrea are with the Department of Engineering, University of Cambridge, Cambridge, CB2 1PZ, UK. (e-mail: akt40@cam.ac.uk).

The remaining sections of this paper are presented as follows; in section II the simulation setup and parameters are stated. In section III the simulation results and discussion are presented and finally in section IV this paper's conclusion is presented.

II. Simulation Setup and Device Design

Three different termination structures are modelled: A Single Zone Junction Termination Extension shown in Fig. *2*, a DZ JTE shown in Fig. 5 and a hybrid DZ JTE SM-FFR shown in Fig. 9. A typical cross-section for the n-IGBT is shown in Fig. 1. The n-drift region, p+ injector and n+ buffer/field stop layers are identical in the active and the termination region of the device. Details on how these meet the requirements for >10kV high temperature operation are discussed in [16].

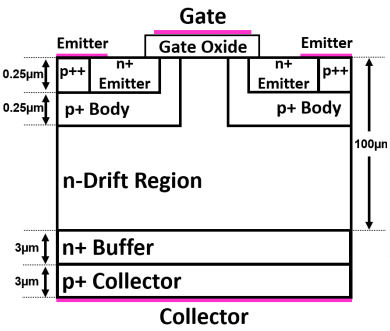

Region	Doping Concentration (cm^{-3})
n+ Emitter	1e18
p++ contact	5e18
p+ Body	1e17
n- Drift	3e14
n+ Buffer	1e18
p+ Collector	1e19

Fig. 1 Cross-sectional schematic of an active planar 4H-SiC n- IGBT and table of doping concentrations

To achieve accurate modelling of the 4H-SiC material performance, accurate and appropriate physics models and parameters need to be used. Unless otherwise specified, the parameters used for this work reflect those in [17]. The phenomenon of impact ionization and therefore, breakdown due to avalanche in this work is modelled with the Okuto-Crowell model as per Eq. (1) and Table 1.

$$\alpha(F_{ava}) = a\left(1 + c(T - T_0)\right)F_{ava}^{\gamma} \exp\left[-\left(\frac{b[1+d(T-T_0)]}{F_{ava}}\right)^{\delta}\right] \quad (1)$$

TABLE I: Okuto-Crowell Avalanche Parameters [18]

Symbol	Electrons	Holes	Unit
A	**$1.43\text{x}10^{5}$**	**$3.14\text{x}10^{6}$**	**V^{-1}**
B	**$4.93\text{x}10^{6}$**	**$1.18\text{x}10^{7}$**	**V/cm**
C	**$6.30\text{x}10^{-3}$**	**$6.30\text{x}10^{-3}$**	**K^{-1}**
D	**$1.23\text{x}10^{-3}$**	**$1.23\text{x}10^{-3}$**	**K^{-1}**
Γ	**0**	**0**	**1**
Δ	**2.37**	**1.02**	**1**

To account for the three-Dimensional junction curvature effect simulations, assume a cylindrical geometry of 120µm and were simulated at 300K.

III. Results and Discussion

A. Single Zone Junction Termination Extension

Fig. 2 illustrates the schematic view of the proposed cross-sectional SZ-JTE termination. The design features a transition region, JTE region, spacer and field stopper.

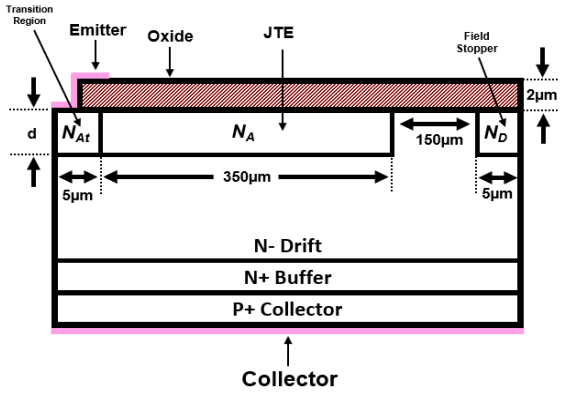

Fig. 2 Cross-sectional schematic of proposed SZ-JTE structure.

The realized breakdown voltage in SZ-JTE structures has a strong dependency on the doping, length and depth of the JTE region [15]. Fig. 3 shows the simulated breakdown voltage as a function of the doping concentration for the conventional SZ JTE structure, the breakdown voltage increases with the JTE doping, reaching a maximum value of 11.6 kV (87% of ideal value) at the JTE doping of $9.5\text{x}10^{16}$ cm^{-3}, and then abruptly decreases with additional the JTE doping.

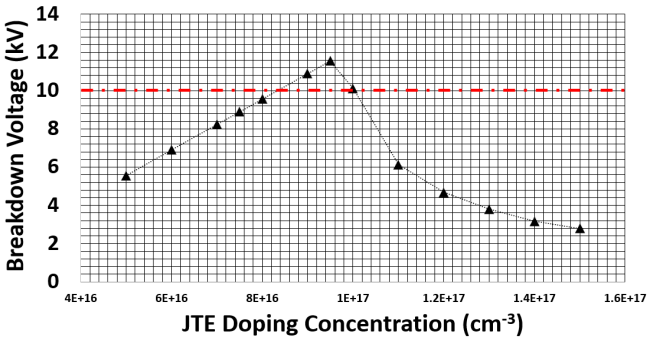

Fig. 3 Blocking Voltage as a function of active doping concentration for the SZ-JTE structure.

The activation of the implanted dopants can fluctuate across the wafer. Also, the exact amount activated is very difficult to control or know in advance. This presents considerable process reliability concerns as small variations in the activated implanted dopants may dramatically reduce the breakdown voltage. It is therefore, desirable to design significantly more robust termination designs which mitigate the fluctuations in the implanted dopants. Hence expanding the doping window is of a primary concern.

The peak blocking capability is achieved when the termination is optimized, i.e. when the peak electric fields are distributed evenly at breakdown. Fig. 4 displays the electric field distribution at the surface and JTE junction for the JTE concentration of $9.5x10^{16}$ cm^{-3} at breakdown.

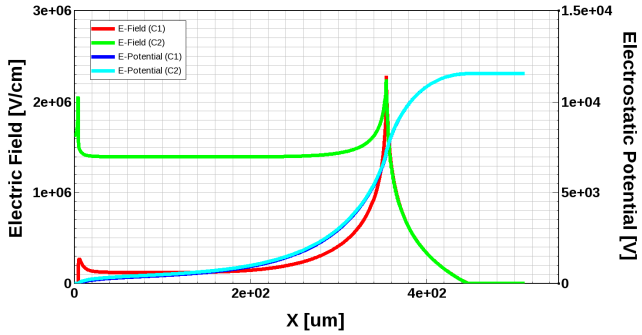

Fig. 4 Electric field distribution for the 9.5x1016 cm-3 concentration for the SZ-JTE structure. C1 is at the surface of the semiconductor, just below the interface with the oxide. C2 is along a Y-cut line that passes from the peak electric field.

As evident from Fig. 4, the maximum electric field is equally distributed between the edge of the transition region and JTE region. Thus, indicating that electric field crowding is significantly higher at these locations. In addition, denoting that any further optimization to improve the design's robustness should be carried out to alleviate the electric field here, one solution is the development of a second JTE region.

Furthermore, Fig. 4 also presents additional concerns into the excessive electric field at the surface which may result in excess leakage current, breakdown walkout and premature breakdown [19].

B. Double Zone Junction Extension Termination

The schematic cross-sectional view of the proposed DZ-JTE structure is shown in Fig. 5. The DZ-JTE is similar to the SZ-JTE presented in Fig. 2 however, the JTE region is split up into two separate regions where JTE1 has a higher doping concentration and longer width than JTE2. The depth of JTE1

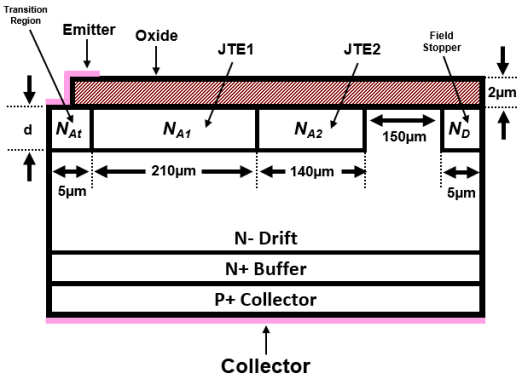

Fig. 5 Cross-sectional of proposed DZ JTE structure.

and JTE2 implantations (d in Fig. 5) is kept at 0.8µm and the total termination length at ~500-510µm. The authors demonstrated with simulations not included in this paper that the ratio of 3:2 of JTE1 and JTE2 yielded the greatest breakdown voltages and the widest possible activated dose window.

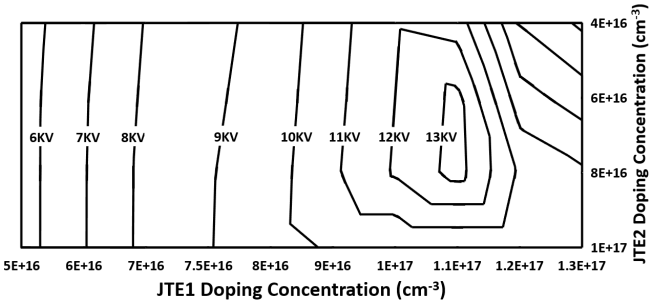

Fig. 6 DZ JTE structure contour plot of BV in kV as a function of the JTE1 doping concentration and JTE2 doping concentration

Fig. 6 is a contour plot displaying the breakdown voltage of the DZ-JTE as a function of the JTE1 and JTE2 doping concentrations. It is clear from Fig. 6 that the maximum breakdown voltage has been increased compared to the single zone, reaching 13.4 kV (99% of ideal value) with a JTE1 doping of $1.1x10^{17}$ cm^{-3} and a JTE2 doping of $8x10^{16}$ cm^{-3}. The proposed DZ-JTE termination design allows a 25% deviation in doping concentrations, whilst still achieving the required blocking voltage of 10kV.

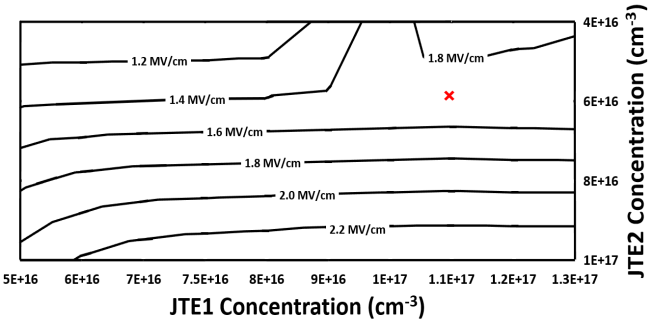

Fig. 7 DZ JTE structure contour plot of Max Electric field in the termination oxide at Breakdown in MV/cm as a function of the JTE1 doping concentration and JTE2 doping concentration.

The peak electric field within the oxide at breakdown for different doping variations for the DZ-JTE is shown in Fig. 7. The electric field contours can be overlapped with those of BV in Fig. 6, to find the optimum DZ-JTE design. There exists a through of electric field strength which covers a range of doping values that also give the desired blocking voltage and high dose window variation. The DZ-JTE termination design achieves >13kV with a doping of JTE1 of $1.1x10^{17}$ cm^{-3} and JTE2 of $8x10^{16}$ cm^{-3} or $6x10^{16}$ cm^{-3} however, $6x10^{16}$ cm^{-3} provides a reduction in the peak electric field in the oxide by over 25% at the cost of ~110V. Therefore, illustrating a trade-off with blocking voltage and the peak

electric field in the termination oxide. The optimum design is the one which sits in the electric field through and it is indicated with an x in Fig. 6. The highest electric field in the oxide is 1.7MV/cm, well below the desired <4MV/cm to ensure reliable operation.

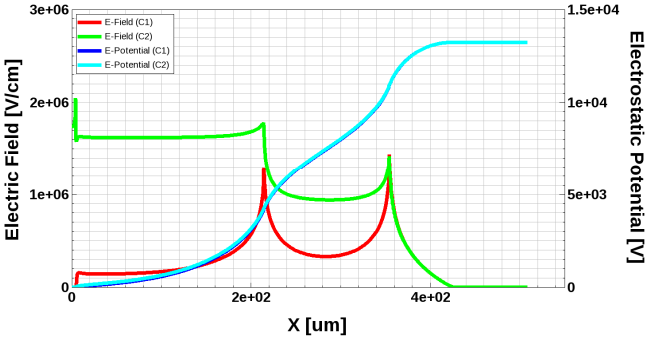

Fig. 8 Electric field distribution for the $1.1x10^{17}$ cm-3 and $6x10^{16}$ cm^{-3} concentration for the DZ-JTE structure.

The electric field distribution at the semiconductor surface and JTE junction for the DZ-JTE with a JTE1 doping of $1.1x10^{17}$ cm^{-3} and JTE2 doping of $6x10^{16}$ cm^{-3} is presented in Fig. 8. The peak electric field is somewhat equally distributed across the DZ-JTE structure, with the transition and JTE2 edges experiencing slightly higher electric field crowding than the edge of JTE1. This suggests that further optimization can be achieved if regions are introduced which supress these peak electric fields. Furthermore, compared to the SZ-JTE the electric field observed at the surface is more evenly distributed across the structure indicating a greater reliability of performance compared to that of the SZ-JTE.

C. Hybrid Double Zone Junction Termination Extension with Space Modulated Floating Field Rings

The cross-sectional view of the proposed Hybrid DZ-JTE SM-FFR structure is shown in Fig. 9. The Hybrid DZ JTE-SM-FFR is identical in dimensions to the DZ-JTE however, it incorporates space modulated floating field rings. Additional simulations not included here were performed for

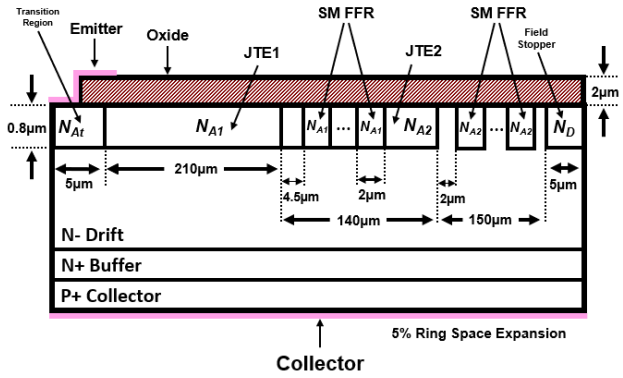

Fig. 9 Cross-sectional of proposed Hybrid DZ-JTE SM-FFRs structure.

the optimization of the hybrid structure. The optimal design requires two different initial ring space, 4.5µm for the first ring space in JTE2 is at 4.5µm and the first ring space in the spacer region, just after the end of JTE2 is 2µm. There exist 10 rings in JTE 2 and 19 in the spacer region. The ring space expansion ratio is 5% which is reset at the end of JTE2.

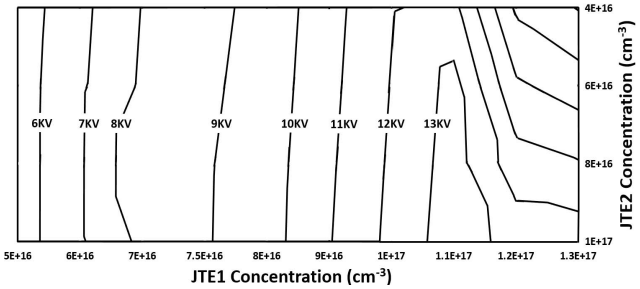

Fig. 10 Hybrid DZ-JTE SM-FFRs structure contour plot of BV in kV as a function of the JTE1 doping concentration and JTE2 doping concentration.

Fig. 10 is a contour plot displaying the breakdown voltage of the Hybrid DZ-JTE SM-FFR structure as a function of the JTE1 and JTE2 doping concentrations. The maximum breakdown voltage is similar to the DZ-JTE structure, achieving maximum value of 13.5 kV (99% of ideal value) with a JTE1 doping of $1.1x10^{17}$ cm^{-3} and a JTE2 doping of $8x10^{16}$ cm^{-3}. In addition, the proposed Hybrid DZ-JTE SM-FFR design allows a 30% deviation in doping concentrations, whilst still achieving the required blocking voltage of 10kV. The Hybrid DZ-JTE SM-FFR introduces additional complexities in the process steps. However, this can be simplified with uniform doping selections for the JTE and ring regions, as simulated in this work.

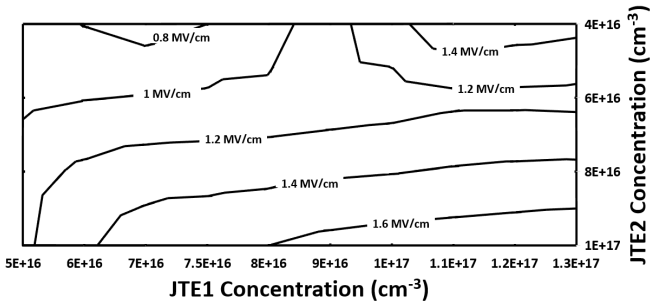

Fig. 11 Hybrid DZ-JTE SM-FFRs structure contour plot of Peak Electric field in the termination oxide at Breakdown in MV/cm as a function of the JTE1 doping concentration and JTE2 doping concentration.

As mentioned before, reductions in the electric field will inevitably produce more reliable performance, particularly if the electric field in the oxide is contained below 4 $MVcm^{-1}$. Fig. 12 shows a significant reduction in the electric field compared to that of the DZ-JTE structure. Like the SZ-JTE the DZ-JTE presents the need for the trade-off of blocking voltage and the peak electric field in the termination oxide to

be considered. This can be again illustrated by choosing a termination design that achieves >13kV. It can be achieved with a doping of JTE1 of $1.1x10^{17}$ cm^{-3} and JTE2 of $8x10^{16}$ cm^{-3} or $6x10^{16}$ cm^{-3} however, $6x10^{16}$ cm^{-3} provides a reduction in the peak electric field in the oxide by approximately 20% at the cost of ~100V.

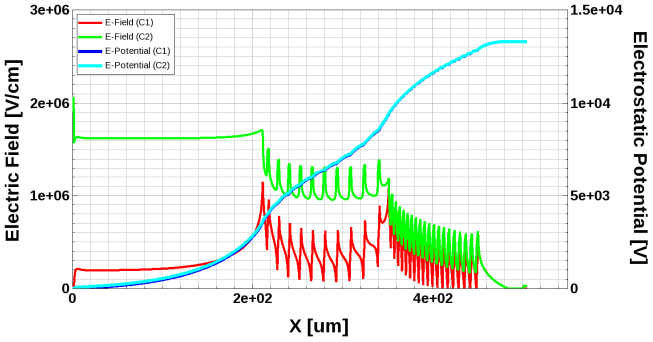

Fig. 12 Electric field distribution for the $1.1x10^{17}$ cm^{-3} and $6x10^{16}$ cm^{-3} concentration for the DZ-JTE structure.

The electric field distribution at the surface and JTE junction for the hybrid DZ-JTE SM-FFR with a JTE1 doping of $1.1x10^{17}$ cm^{-3} and JTE2 doping of $6x10^{16}$ cm^{-3} is presented in Fig. 12. The peak electric fields are distributed over the JTE and FFR edges across the termination structure, with the transition edge experiencing highest electric field, suggesting significant crowding occurs at that point. The surface electric field is largely distributed across the latter part of the structure and subsequently a ~50% is seen compared to that of the DZ-JTE.

IV. Conclusion

In this paper, we have presented three optimized termination designs which enable the fabrication of a >10kV n-IGBT. We emphasized and demonstrated the electric field in the termination oxide can be significantly supressed with the choice of termination design and appropriate doping concentrations, without significant reductions in the termination's blocking capabilities. We showed that the DZ-JTE and the Hybrid DZ-JTE SM-FFR with JTE1 at $1.1x10^{17}cm^{-3}$ and JTE2 at $6x10^{16}cm^{-3}$ can supress the peak electric field in the termination oxide by 25% and 20% respectively, whilst only sacrificing ~1% of blocking ability. Indeed, as shown in this work, sole optimization of blocking voltage and doping concentration window will not provide the most optimal termination design for reliability.

References

[1] E. van Brunt *et al.*, "27 kV, 20 A 4H-SiC n-IGBTs," *Mater. Sci. Forum*, vol. 821–823, pp. 847–850, 2015.

[2] E. V. Brunt *et al.*, "22 kV, 1 cm2, 4H-SiC n-IGBTs with improved conductivity modulation," *Proc. Int. Symp. Power Semicond. Devices ICs*, no. c, pp. 358–361, 2014.

[3] S. H. Ryu *et al.*, "Development of 15 kV 4H-SiC IGBTs," *Mater. Sci. Forum*, vol. 717–720, pp. 1135–1138, 2012.

[4] M. K. Das *et al.*, "A 13 kV 4H-SiC n-Channel IGBT with Low Rdiff,on and Fast Switching," *Mater. Sci. Forum*, vol. 600–603, pp. 1183–1186, 2009.

[5] J. Senzaki, S. Hayashi, Y. Yonezawa, and H. Okumura, "Challenges to realize highly reliable SiC power devices: From the current status and issues of SiC wafers," *IEEE Int. Reliab. Phys. Symp. Proc.*, vol. 2018–March, p. 3B.31-3B.36, 2018.

[6] D. Alok, P. K. McLarty, and B. J. Baliga, "Electrical properties of thermal oxide grown using dry oxidation on p-type 6H-silicon carbide," *Appl. Phys. Lett.*, vol. 65, no. 17, pp. 2177–2178, 1994.

[7] M. E. Levinshtein, S. L. Rumyantsev, M. Shur, V. Bougrov, and A. Zubrilov, *Properties of Advanced Semiconductor Materials: GaN, AIN, InN, BN, SiC, SiGe*. 2001.

[8] R. Singh, "Reliability and performance limitations in SiC power devices," *Microelectron. Reliab.*, vol. 46, no. 5–6, pp. 713–730, 2006.

[9] R. Degraeve, J. L. Ogier, R. Bellens, P. J. Roussel, G. Groeseneken, and H. E. Macs, "A new model for the field dependence of intrinsic and extrinsic time-dependent dielectric breakdown," *IEEE Trans. Electron Devices*, vol. 45, no. 2, pp. 472–481, 1998.

[10] Y. Gao, S. I. Soloviev, T. S. Sudarshan, I. I. Khlebnikov, and Y. I. Khlebnikov, "Aluminum and Boron Diffusion into (1-100) Face SiC Substrates," *Mater. Sci. Forum*, vol. 389–393, pp. 557–560, 2009.

[11] H. Niwa, J. Suda, and T. Kimoto, "Fundamental study on junction termination structures for ultrahigh-voltage SiC PiN diodes," *IMFEDK 2012 - 2012 Int. Meet. Futur. Electron Devices, Kansai*, no. 21226008, pp. 56–57, 2012.

[12] W. Sung and B. J. Baliga, "A Comparative Study 4500-V Edge Termination Techniques for SiC Devices," *IEEE Trans. Electron Devices*, vol. 64, no. 4, pp. 1647–1652, 2017.

[13] G. Feng, J. Suda, and T. Kimoto, "Space-modulated junction termination extension for ultrahigh-voltage p-i-n diodes in 4H-SiC," *IEEE Trans. Electron Devices*, vol. 59, no. 2, pp. 414–418, 2012.

[14] R. Pérez, D. Tournier, A. Pérez-Tomas, P. Godignon, N. Mestres, and J. Millán, "Planar edge termination design and technology considerations for 1.7-kV 4H-SiC PiN diodes," *IEEE Trans. Electron Devices*, vol. 52, no. 10, pp. 2309–2316, 2005.

[15] A. Mahajan and B. J. Skromme, "Design and optimization of junction termination extension (JTE) for 4H-SiC high voltage Schottky diodes," *Solid. State. Electron.*, vol. 49, no. 6, pp. 945–955, 2005.

[16] S. Perkins *et al.*, "The Development of UHV 4H-SiC n-IGBT for high Temperature Environments," *ISPS*, 2018.

[17] N. Lophitis, A. Arvanitopoulos, S. Perkins, and M. Antoniou, *TCAD device modelling and simulation of wide bandgap power semiconductors*. InTech – Open Access Publisher, 2018.

[18] W. S. Loh *et al.*, "Impact ionization coefficients in 4H-SiC Ultrahigh-Voltage Power Devices," *IEEE Trans. Electron Devices*, vol. 55, no. 8, pp. 1984–1990, 2008.

[19] G. Feng, J. Suda, and T. Kimoto, "Space-modulated junction termination extension for ultrahigh-voltage p-i-n diodes in 4H-SiC," *IEEE Trans. Electron Devices*, vol. 59, no. 2, pp. 414–418, 2012.

AUTHORS' INFORMATION

Samuel Perkins was born in Norwich in the United Kingdom, on September 17th, 1993. He received his B.Eng. and MRes degrees from Coventry University, Coventry, in 2017. Currently he is pursuing his PhD degree at Coventry University. His research is focused on Wide Bandgap (WBG) power semiconductor devices for Ultra High Voltage applications. Of his particular interest is the physical modelling of WBG semiconductor materials and characterisation of 4H-SiC n-IGBTs for Ultra High Voltage applications.

Marina Antoniou received the B.A. and M. Eng. degrees in electrical and information engineering from the University of Cambridge (Trinity College), Cambridge, U.K., and the Ph.D. degree in electrical engineering from Cambridge. She was a Junior Research Fellow in Selwyn College, Cambridge, U.K. She is currently an Associate Professor at the University of Warwick and is also affiliated with the U.K. Power Electronics Centre. Her research interests include power electronics and high voltage power semiconductor devices.

Amit K. Tiwari is a Research Associate in the Department of Engineering of University of Cambridge, having received his PhD degree from Newcastle University in 2013, and MTech degree from Indian Institute of Technology Delhi, India, in 2009. Dr. Tiwari's primary research interests lie with advanced wide bandgap semiconductors including SiC and diamond. His area of expertise is design-characterization of ultra-high voltage power devices. Over the last 8 years, he has extensively researched Bi-directional Current Limiting Diodes, Solid-State Damping Resistors, High-mobility MOSFETs and IGBTs. Dr. Tiwari has published over 25 articles in peer-reviewed journals and conference proceedings. He has given a number of invited talks, including winning the best presentation award at the DeBeers Diamond Conference (2012). He is the recipient of prestigious EPSRC-Dorothy Hodgkin Postgraduate Award in 2009 in the UK and the CSIR-Junior Research Fellowship in 2007 in India.

Arvanitopoulos E. Anastasios was born in Patras, Greece, in May 1985. He received the Diploma in Electrical and Computer Engineering from the University of Patras, Greece in 2011. Since October of 2016 he has been a Ph.D. Candidate at the Research Institute for Future Transport and Cities, Coventry University, UK. His research is focused on Wide Bandgap (WBG) power semiconductor devices for high performance electronics in Electric Vehicles (EVs). Of his particular interest is the physical modelling of WBG semiconductor materials and devices aiming to accurately simulate the effect of defects in the device operation.

Konstantinos N. Gyftakis (M'11) was born in Patras, Greece, in May 1984. He received the Diploma in Electrical and Computer Engineering from the University of Patras, Patras, Greece in 2010. He pursued a Ph.D in the same institution in the area of electrical machines condition monitoring and fault diagnosis (2010-2014). Then he worked as a Post-Doctoral Research Assistant in the Dept. of Engineering Science, University of Oxford, UK (2014-2015). Then he worked as Lecturer (2015-2018) and Senior Lecturer (2018-2019) in the School of Computing, Electronics and Mathematics and as an Associate with the Research Institute for Future Transport and Cities, Coventry University, UK. Additionally, since 2016 he has been a member of the "Centro de Investigação em Sistemas Electromecatrónicos" (CISE), Portugal. Since 2019 he has been a Lecturer in Electrical Machines, University of Edinburgh, UK. He has authored/co-authored more than 70 papers in international scientific journals and conferences and a chapter for the book: "Diagnosis and Fault Tolerance of Electrical Machines, Power Electronics and Drives", IET, 2018.

Tatjana Trajkovic received a PhD degree in Engineering from King's College, University of Cambridge. She has more than 15 years of experience in development of high voltage lateral power devices and Power ICs as well as vertical IGBTs rated up to 6.5kV. She joined CamSemi as one of the founding members where she worked for 10 years. She has published more than 30 papers and is the co-inventor of 7 patents and patent applications. She has a proven record in taking new technologies and product ideas from concept through qualification to volume manufacturing. She has experience with academic and commercial environments, small and dynamic start-ups and multinational companies.

Florin Udrea (M'91) received the Ph.D. degree in power devices from the University of Cambridge, Cambridge, U.K., in 1995. He is currently a Professor of semiconductor engineering and the Head of the High Voltage Microelectronics and Sensors Laboratory, University of Cambridge. He has authored more than 400 papers published in journals and international conference proceedings. He holds 70 patents with 20 more patent applications in power semiconductor devices and sensors. He cofounded three companies, Cambridge Semiconductors (Camsemi) in power ICs, Cambridge CMOS Sensors (CCS) in the field of smart sensors, and Cambridge Microelectronics in power devices. He is also a Board Director at Cambridge Enterprise. Prof. Udrea received the Silver Medal from the Royal Academy of Engineering for his outstanding personal contribution to British engineering.

Neophytos Lophitis received the B.A. and M.Eng. degrees in 2009 and the Ph.D. degree in Power Devices in 2014, all from the University of Cambridge. Then he worked as a Research Associate in Power at the University of Cambridge (2014-15) and as a consultant for Power Microelectronics companies (2013-15). He joined Coventry University in 2015 where he is currently an Assistant Professor of Electrical Engineering at the School of Computing, Electronics & Mathematics and the research Institute for Future Transport and Cities. Since 2015 he has also been a member of the "High Voltage Microelectronics Laboratory" at the University of Cambridge, UK. Neophytos is also affiliated with the U.K. Power Electronics Centre and the European Centre for Power Electronics. His research includes optimization, design, degradation and reliability of high voltage microelectronic devices and electrical energy storage and conversion systems. He authored/co-authored more than 45 scientific manuscripts, including one book chapter for the book: "Disruptive Wide Bandgap Semiconductors, Related Technologies, and Their Applications", IntechOpen, 2018.